Effects of Compressibility on the Characteristics of Free Shear Layers

M. Samimy* and G. S. Elliott†
Ohio State University, Columbus, Ohio

A high Reynolds number two-dimensional constant pressure compressible shear layer was formed at the trailing edge of a 0.5 mm-thick splitter plate. Convective Mach numbers of 0.51 and 0.64 were investigated using a two-component coincident LDV for the measurements. For the lower convective Mach number case, the nondimensionalized shear-layer and vorticity thickness growth rates were over 20% higher and the momentum thickness growth rate was over 30% higher than those of the higher convective Mach number case. Scaling the lateral dimension of shear layer with the local vorticity thickness collapsed all the mean velocity results for available convective Mach numbers between 0 and 1 from these experiments and the experiments of other investigators. However, when using the local momentum thickness instead of the vorticity thickness, a convective Mach number dependent linear transformation was necessary to collapse the velocity profiles. The lateral turbulence intensity, shear stress, and lateral transport of kinetic energy all nondimensionalized, with the velocity difference across the shear layer showing reduced levels for the higher convective Mach number case. The results seem to indicate that both small scale and large scale mixing are reduced with increasing convective Mach number.

Nomenclature

b = shear layer thickness, between $0.1U^*$ and $0.9U^*$
C_1 = lateral scale transformation coefficient; Eq. (5)
C_2 = lateral scale transformation coefficient; Eq. (6)
M = Mach number
M_c = convective Mach number
R_{uv} = correlation coefficient
U = streamwise mean velocity
U^* = $(U - U_2)/(U_1 - U_2)$
u = streamwise velocity fluctuations
v = lateral velocity fluctuations
x = axial location from trailing edge of the splitter plate
y = vertical location from top surface of the splitter plate
y_0 = the location where $U = (U_1 + U_2)/2$
y_1^* = $(y - y_o)/\theta$
y_2^* = $(y - y_o)/\delta_w$
δ_w = vorticity thickness; Eq. (4)
θ = momentum thickness; Eq. (3)
ρ = density
σ = spread rate
σ_u = streamwise turbulence intensity
σ_v = lateral turbulence intensity

Subscripts

c = compressible
i = incompressible
1 = top stream; Fig. 1
2 = bottom stream; Fig. 1

Introduction

IT has been known for many years that the growth and entrainment rates of compressible free shear layers are much smaller than those of incompressible free shear layers.[1] Initially, it was believed that the significant density change across compressible free shear layers was the cause of these differences. However, experimental investigations of heterogeneous incompressible free shear layers revealed that the density changes across free shear layers play a role, but not a significant enough role to cause the observed differences.[2] Due to the recent revival of research on the hypersonic airbreathing vehicle with a supersonic propulsion system, compressible free shear layers have been under intense scrutiny for the past few years and more information is becoming available. Recent results show that the compressibility, rather than just the density change across free shear layers, is the main cause of lower growth rates in compressible shear layers.[3-9]

Recently, a convective Mach number—a Mach number with respect to a frame of reference travelling with the average large scale structures in the flow—has been identified as the compressibility factor.[3-9] The convective Mach number of both streams are the same, if they have the same specific heats ratio, and is defined as $M_c = (U_1 - U_c)/a_1$, where $U_c = (a_1 U_2 + a_2 U_1)/(a_1 + a_2)$ and a is the speed of sound. Experimental results show a good correlation between the convective Mach number and the compressible free shear-layer growth rate nondimensionalized with the incompressible shear-layer growth rate with the same density and velocity ratios across the shear layers.[3-6] Also, linear inviscid stability analysis shows a similar correlation between the ratio of maximum growth rates of stability waves and the convective Mach number based on a frame of reference travelling with the stability waves.[7-9]

The work presented in this paper is part of ongoing research to investigate the effects of compressibility on the growth rate, mean flow characteristics, and turbulence structure of shear layers. The next section will provide some background information on incompressible and compressible shear layers. Then, the experimental facility and instrumentation will be presented, followed by the experimental results and discussions.

Background

In a configuration similar to the one shown in Fig. 1, Schlichting utilized Gortler's analysis, which assumes a constant eddy viscosity across the incompressible turbulent free-shear layer, and obtained the following solution for the

Received Oct. 26, 1988; revision received April 10, 1989.

*Assistant Professor, Department of Mechanical Engineering. Member AIAA.
†Graduate Student, Department of Mechanical Engineering.

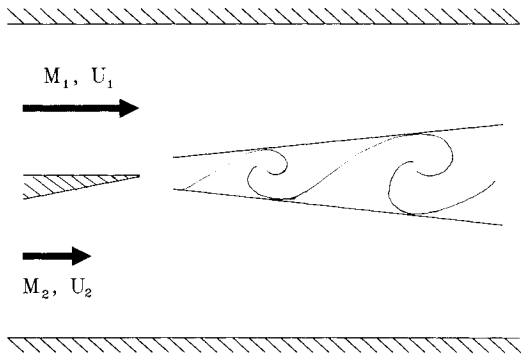

Fig. 1. Schematic of the flowfield.

velocity in the fully developed region of the flow[10]

$$U^* = \frac{U - U_2}{U_1 - U_2} = \frac{1}{2}(1 + erf\eta) \tag{1}$$

where $\eta = \sigma(y - y_o)/(x - x_o)$. In this equation there are three parameters determined experimentally: σ, the spread rate parameter; x_o, the location of the virtual origin; and y_o, the location of $U = (U_1 + U_2)/2$. Many experimental results show that for incompressible flows[1]:

$$\frac{\sigma_0}{\sigma} = \lambda = \frac{U_1 - U_2}{U_1 + U_2} \tag{2}$$

where σ_o is the spread rate parameter for a single flow case ($U_2 = 0$). The values of σ_o have been reported anywhere from 6 to 12, with the majority of data falling between 10 and 11.[1,3,5] These variations could be caused by many variables, such as experimental uncertainties, incoming flow conditions, experimental geometry, different methods of obtaining the spread rate, and many other factors. Also, for single stream supersonic free shear layers, it has been shown that the spread rate parameter increases with the Mach number.[1]

In the fully developed region of a free shear layer, the shear-layer thickness can be written as $b = (x - x_o)/\sigma$. Therefore, rather than determining x_o and σ from experimental results, one needs to determine b, which is a function of x. It is interesting to see how many different ways the shear-layer thickness b has been defined in the literature.[1,3-6,11]

Two other measures of shear-layer thickness are momentum and vorticity thicknesses. Following Oster and Wygnanski,[11] Petrie et al.[12] and Brown and Roshko,[2] we defined the momentum and the vorticity thicknesses of the shear layer as:

$$\theta = \int_{-\infty}^{+\infty} \frac{\rho}{\rho_1} U^*[1 - U^*]\, dy \tag{3}$$

$$\delta_\omega = \frac{U_1 - U_2}{[\partial U/\partial y]_{max}} \tag{4}$$

and used these measures instead of the shear-layer thickness b. In defining a parameter to describe the thickness of the shear layer, two factors should be considered: the number and reliability of the data points used in calculating the thickness, and the ability of the parameter to describe variations in the thickness due to the flow characteristic changes. Using these thickness definitions, instead of the shear-layer thickness, the total number of data points in defining the thickness is increased. Momentum thickness is an integral of all points, and vorticity thickness is calculated from a curve fit of the velocity profile's linear region. The shear-layer thickness b, on the other hand, uses only edge velocities, which can introduce large errors due to very slow changes in velocity profiles at the edge of the shear layer. In both incompressible[1,11,13,14] and compressible[12,15] free shear layers, the momentum thickness has been shown to grow linearly in the fully developed region of the shear layer. The present results confirm this and show that the vorticity thickness also grows linearly.

Using the above thickness definitions, we defined two similarity parameters as

$$\eta_1 = C_1 \frac{y - y_{0.5}}{\theta} \tag{5}$$

$$\eta_2 = C_2 \frac{y - y_{0.5}}{\delta_\omega} \tag{6}$$

and used experimental data from various works with different convective Mach numbers to find C_1 and C_2. In light of the recent concept of convective Mach number, it was expected that the transformation coefficients C_1 and C_2 would be a function of convective Mach number. One goal of the work was to find C_1 and C_2 and then utilize the similarity coordinate system to investigate the effects of convective Mach number on the turbulence characteristics of free shear layers.

Experimental Facility and Instrumentation

Wind Tunnel

The experiments were conducted at the Ohio State University Aeronautical and Astronautical Research Laboratory (AARL). The newly refurbished high Reynolds number supersonic blowdown tunnel is a dual-stream tunnel with a 152.4 × 152.4 mm test section. In the present configuration, the top stream has a nominal Mach 2 nozzle and the bottom stream has a converging nozzle. The 3.175 mm-thick steel splitter plate is flat on the supersonic side and is machined on the subsonic side with approximately 1 degree angle over 125 mm length to about 0.5 mm thickness at the trailing edge. The combination of an interchangeable glass window and an access panel provides an approximately 80 mm high and 500 mm long viewing area, including a 20 mm long section of the incoming boundary layers.

At AARL, the cold and dry air generated at 16.4 MPa (2400 psi) by two four-stage compressors is stored in two storage tanks with 42.5 m^3 (1500 ft^2) capacity. The air is fed into the tunnel by two separate control valves; therefore, flow to both streams can independently be controlled. The tunnel can be operated in a steady-state mode with a mass flow rate of over 18 kg/s for over 90 seconds.

LDV System

A two-component coincident laser Doppler velocimetry system, set at 10 degree off-axis forward scatter mode, was used in these experiments. The measurement volume diameter and length, to e^{-2} intensity level, were 0.13 mm and 0.90 mm, respectively. Two components of LDV were set at ±45 degrees relative to the mean flow direction. Both flows were seeded in the settling chamber with atomized silicone oil less than 1 micron in diameter.[16]

All the LDV results presented here are based on 2048 samples per channel and corrected for velocity bias, using the inverse of total instantaneous velocity as the weighting factor in the statistical analysis. Since there is no zero or near zero instantaneous total velocity in the flowfield under study, this scheme is a suitable and convenient technique.[17,18] Although the number of samples taken are sufficient for mean velocity results, a larger sample size would be desirable to reduce the scatter in the turbulence results.

Experimental Results and Discussions

Incoming Boundary Layers

The incoming supersonic flow was a Mach 1.83 fully developed turbulent boundary layer with the boundary layer and

the momentum thicknesses of approximately 8 mm and 0.5 mm, respectively. The stagnation pressure and temperature were approximately 314 kPa and 291 ± 3% K. Variations in the stagnation temperature were mostly due to the ambient temperature change. The Reynolds number based on the momentum thickness was approximately 21,500.

Figure 2 presents the profiles of mean streamwise velocity and turbulence fluctuations, both normalized with the freestream velocity, 492 m/s, and the correlation coefficient, R_{uv}. The turbulence intensity profile with approximately 7.5% maximum intensity level at $y/\delta = 0.3$ is similar to both subsonic and supersonic turbulent boundary layer profiles reported by many other investigators.[12] The general trend of correlation coefficient is similar to subsonic and supersonic boundary-layer results. The magnitudes of the correlation coefficient agree well with the supersonic results and are approximately 15% lower than the subsonic values.[19,20]

The two convective Mach number cases were obtained by operating the incoming subsonic flow at Mach numbers of 0.51 and 0.37. For the first case (case 1), the matched static pressure case, the supersonic stream fully expanded at the edge of the splitter plate, thus generating a very weak expansion or compression wave due to the boundary-layer displacement thickness and the finite thickness of the splitter plate trailing edge. The convective Mach number of the mixing layer for this case was 0.51. For the second case, the underexpanded case, the supersonic stream passed through a centered expansion wave at the trailing edge of the splitter plate. The convective Mach number for this case was 0.64.

Pressure Measurements and Flow Visualizations

The static pressures in the test section were measured by pressure taps on the top and the bottom walls of the tunnel and also on the plexiglass windows. The plexiglass windows replaced the glass windows for the pressure measurements. For the matched pressure case, in the entire viewing area, and for the underexpanded case, in the region before the expansion waves generated at the trailing edge of the splitter plate reflecting off the top wall and interacting with the shear layer ($x < 250$ mm), the pressure variation was within 6% of the mean pressure.

A standard Schlieren system with a 500 ns flash duration was utilized for flow visualization. The photographs for case 1 showed a small narrow wake extending approximately 10 mm behind the splitter plate and the incoming boundary layer riding on the developing shear layer and getting engulfed by the shear layer. By approximately $x = 80$ mm, the shear layer had totally engulfed the incoming boundary layer. Some photographs obtained recently by using an argon laser-based Schlieren system and a newly acquired intensified CCD camera with a 10 ns flash duration showed the existence of large scale structures. The structures do not seem to be that organized and appear very randomly, but they seem to be similar to those observed in supersonic reattaching shear layers[21] and supersonic boundary layers.[22]

Mean Flow Results

As discussed earlier, two convective Mach number cases were investigated. Table 1 shows the pertinent parameters for each case. The parameters C_1, C_2, and the data for Refs. 11 and 15 will shortly be discussed.

In order to find the effects of convective Mach number on the transformation coefficients C_1 and C_2 in Eqs. (5) and (6) in a more general sense, we will describe the steps taken for finding C_1 and then apply them to C_2. First, the subsonic mean velocity profiles from Oster and Wygnanski,[11] in a configuration similar to the one shown in Fig. 1 with velocity ratios of 0.3, 0.4, 0.5, and 0.6, were taken and plotted in U^* vs the y_1^* coordinates. This subsonic data collapsed on a single curve. Next, the present data and the data from Ikawa and Kubota[15] were plotted on the same graph (Fig. 3). Notice in Fig. 3 that the slope of the linear portion of the profile decreases as the convective Mach number increases. Therefore, the transformation coefficient C_1 in Eq. (5) (determined through curve fitting) is introduced to collapse the data, using the subsonic profile as a reference (Fig. 4). In order to make the graph less crowded, only one profile in the fully developed region is shown for each case. As shown in Table 1, the transformation coefficient C_1 is a function of convective Mach number and decreases as the convective Mach number increases. In fact, the relation in the range of M_c from 0 to 1 seems to be linear; $C_1 = 1.0 - 0.41M_c$.

The same analysis was done using vorticity thickness as the transverse normalization factor, as shown in Eq. (6). Figure 5 shows U^* vs y_2^* in five streamwise locations for case 1 and four locations for case 2. Except for case 1 at $x = 60$ mm, all the profiles collapse on a single curve. This indicates that both cases reached self-similarity, at least in the mean flow sense, for $x \geq 120$ mm or $x/\Theta \geq 240$. (It will be shown later that turbulence self-similarity is reached further downstream.) The collapsed results also indicate that C_2 is independent of the convective Mach number (since it is unity throughout) and can be eliminated from the similarity definition in Eq. (6). Figure 6 shows the profiles from the two present cases, along with available profiles from other investigators (Refs. 3, 5, 11, and 15) plotted on the same graph, with y_2^* as the abscissa. Note again the results collapse within expected experimental accuracy, indicating that C_2 is unity.

Since both $C_1 y_1^*$ and y_2^* scales collapse all the data for different M_c and are related by a constant ($y_2^* = 0.18 C_1 y_1^*$), either scale could be used to investigate the effects of convective Mach number on the turbulence characteristics. In the results to follow, y_2^* will be used.

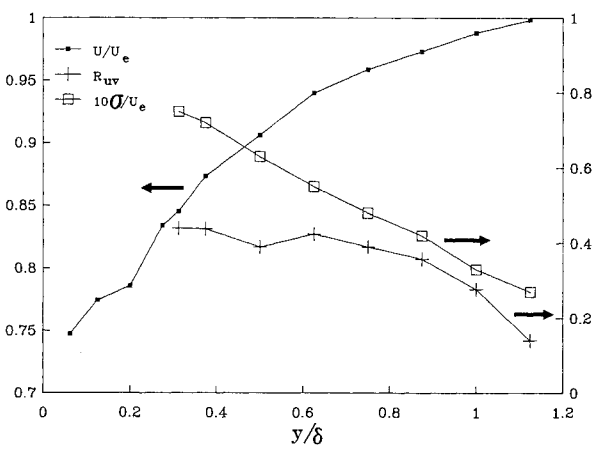

Fig. 2. The incoming boundary-layer results.

Table 1 Mean flow parameters

Source	M_1	M_2	M_c	U_2/U_1	ρ_2/ρ_1	C_1[Eq.(4)]	C_2[Eq.(5)]
Ref. 11	0.0	0.0	0.0	0.3, 0.4 0.5, 0.6	1.0	1.0	1.0
Case 1	1.80	0.51	0.51	0.36	0.64	0.80	1.0
Case 2	1.96	0.37	0.64	0.25	9.58	0.74	1.0
Ref. 15	2.47	0.0	1.0	0.0	0.45	0.58	1.0

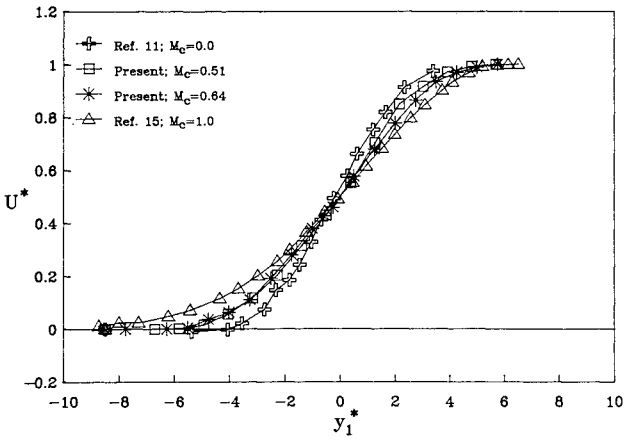

Fig. 3. Axial mean flow profiles from various experiments with y_1^* as the lateral scale.

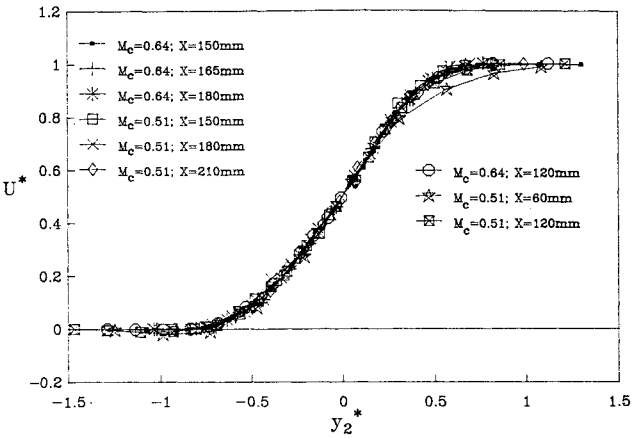

Fig. 5. The axial mean flow velocities of cases 1 and 2 with y_2^* as the lateral scale.

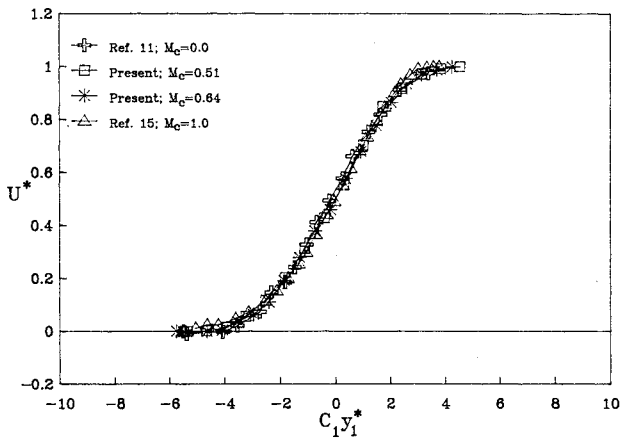

Fig. 4. Axial mean flow profiles from various experiments with $C_1 y_1^*$ as the lateral scale.

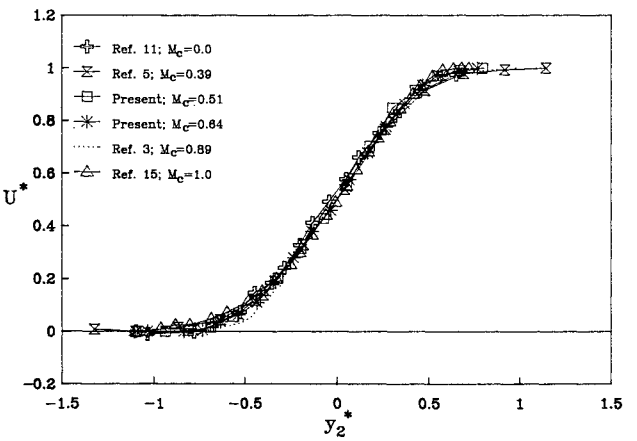

Fig. 6. Axial mean flow profiles from various experiments with y_2^* as the lateral scale.

Many researchers have used hyperbolic tangent type, rather than error function type, mean velocity profiles in the stability analysis of supersonic shear layers.[7,8] The following expressions were obtained through curve fitting of the experimental results in Figs. 4 and 6. These expressions should be useful in the analytical and computational studies.

$$U^* = \frac{1}{2}[1 + \tanh(0.43 C_1 y_1^*)] \tag{7}$$

$$U^* = \frac{1}{2}[1 + \tanh(2.4 y_2^*)] \tag{8}$$

Shear-Layer Growth and Entrainment Rates

As was discussed, it has been known for many years that the growth rate of compressible shear layers is smaller than that of the incompressible shear layers, with the same velocity and density ratios across the shear layers. Recently, a trend has been established that shows the convective Mach number correlates this growth rate ratio.[3-6] Figure 7 shows the shear-layer thickness defined as the thickness between $U^* = 0.1$ and 0.9, the momentum thickness, and the vorticity thickness as defined in Eqs. (3) and (4), respectively. Beyond $x = 120$ mm, all the shear-layer mixing rate measures show linear growth. Using linear regression, the growth rates for these thickness definitions were calculated and are shown on Fig. 7.

Figure 8 shows the growth rate of supersonic shear layers for the present experiments and some other selected references. The growth rate is nondimensionalized, with the growth rate of incompressible shear layers determined by using Eq. (2) with $\sigma_o = 10$. Figure 5 of Ref. 5 shows a significant scatter in σ_o from many different experiments. The results in Fig. 8 show a definite trend; however, the data is scattered significantly due to, as was mentioned earlier, experimental uncertainties, influence of incoming flow conditions, different experimental geometries, different methods of determining the spread rate, reliability of the edge velocities in determining the thickness, and many other parameters.

The momentum thickness defined in Eq. (3) is perhaps a better physical representative of the shear-layer mixing. One can show that the momentum thickness growth rate is closely related to shear-layer entrainment rate.[12] Oster and Wygnanski's results show that for their subsonic shear layers $d\theta/dx = 0.035\lambda$ for four different velocity ratios. This relation was used to calculate $d\theta/dx$ for incompressible shear layers. Table 2 indicates the significant effects of convective Mach number on the entrainment rate ratio of compressible to incompressible free shear layers.

The mean flow results in Fig. 6 show that the vorticity thickness is the best lateral length scale and perhaps a better measure of the gross mixing rate. For subsonic shear flows, Brown and Roshko[2] have shown that $d\delta_w/d(x - x_o) = 0.181(U_1 - U_2)/(U_1 + U_2)$. Bogdanoff[9] used this relation to nondimensionalize the vorticity growth rate for different convective Mach numbers from various experiments. Figure 9 is taken from Bogdanoff. As can be seen, the present results agree very well with the results from other researchers.

Turbulence Results

The collapse of mean velocity profiles with different convective Mach numbers in Figs. 4 and 6 is a good indication that

$(U_1 - U_2)$ and y_2^* (or $C_1 y_1^*$) are the proper scaling parameters. These parameters will be used to compare the turbulence characteristics of compressible and incompressible shear layers and to determine the effects of convective Mach number on the turbulence characteristics. The mean flow results in Fig. 5 showed that both cases of the present study were fully developed in the mean flow sense for $x \geq 120$ mm. However, within the accuracy of the experimental results, the data for each case of the present experiments seemed to collapse only for $x \geq 150$ mm, which showed that the turbulence similarity was achieved further downstream than the mean flow similarity, as expected.

Figure 10 shows streamwise turbulence fluctuation of present experiments for the fully developed region ($x \geq 150$ mm) and the incompressible results of Oster and Wygnanski.[11] Oster and Wygnanski's results for four different velocity ratios from Figs. 6a–d of their paper were first replotted and observed to collapse on a single curve. Thus, only a single curve for their result is shown in Fig. 10. The compressibility seems to reduce the maximum fluctuations that occur around $y_2^* = 0$ for both compressible and incompressible flows. The maximum fluctuations for incompressible

Table 2 Growth rate results

	M_c	$d\theta/dx$	$(d\theta/dx)_c/(d\theta/dx)_i$
Case 1	0.51	0.0159	0.96
Case 2	0.64	0.0137	0.65
Ref. 15	1.0	0.0073	0.20

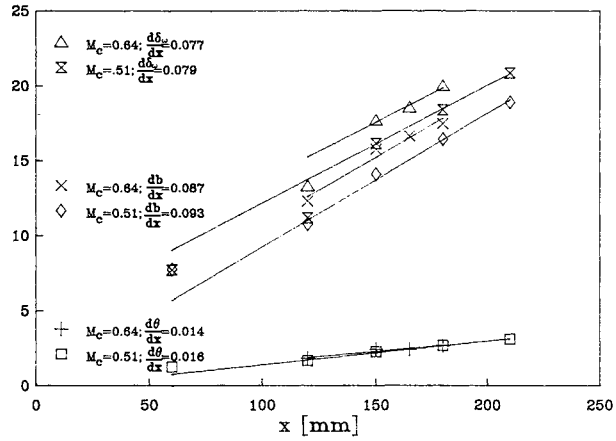

Fig. 7. Shear-layer, momentum, and vorticity thicknesses.

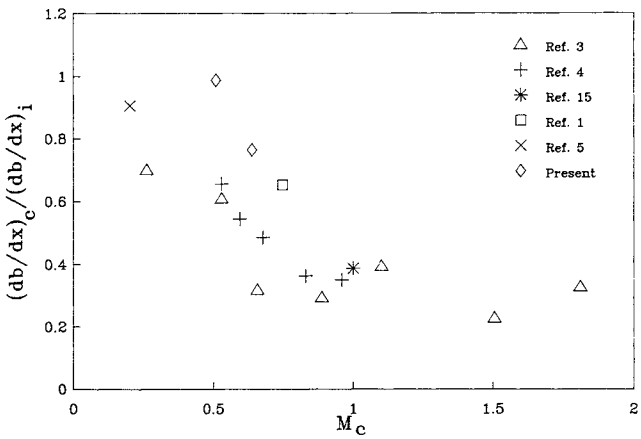

Fig. 8. Shear-layer growth rate from various experiments.

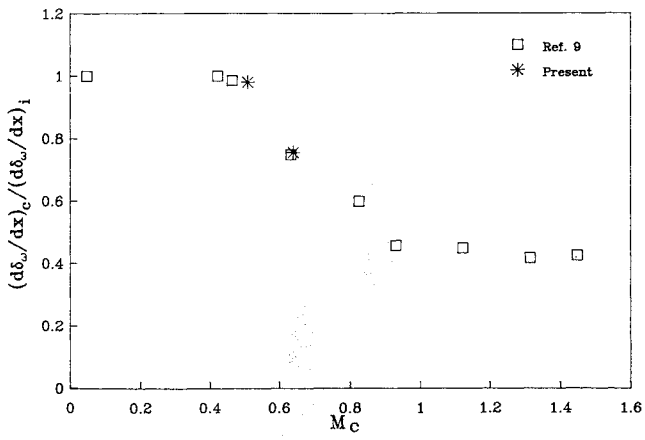

Fig. 9. Vorticity growth rate for various experiments.

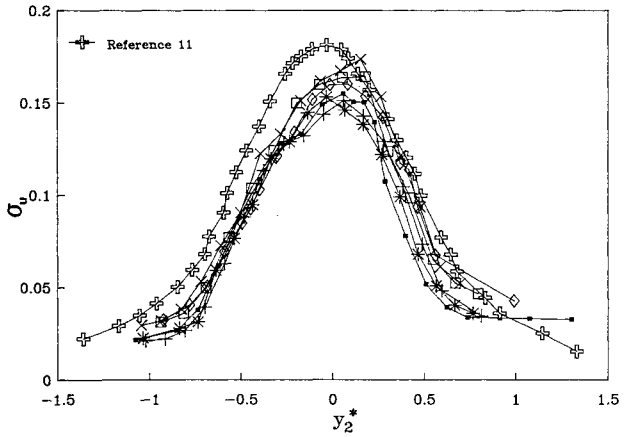

Fig. 10. Streamwise turbulence intensities.

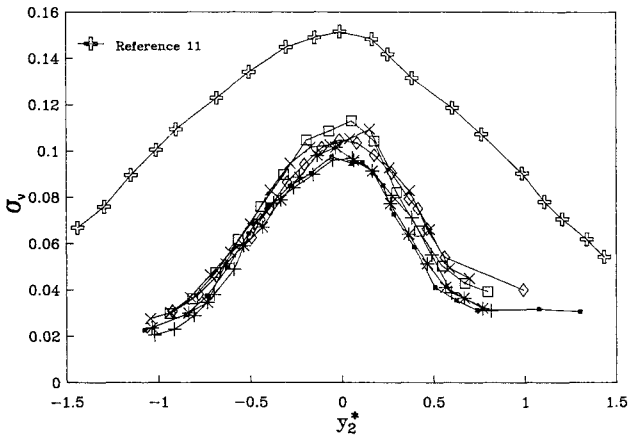

Fig. 11. Lateral turbulence intensities.

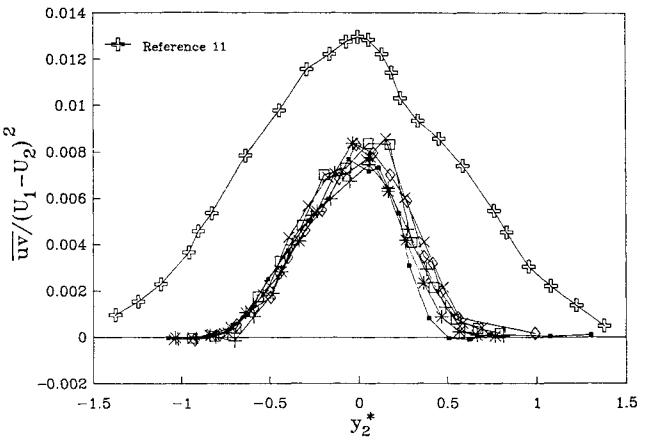

Fig. 12. The Reynolds stress profiles.

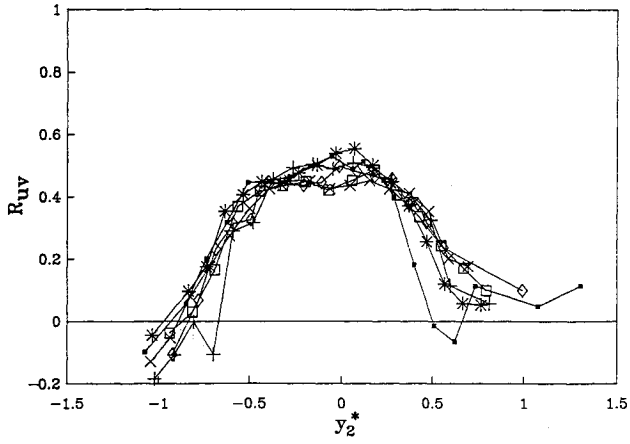

Fig. 13. The correlation coefficient profiles.

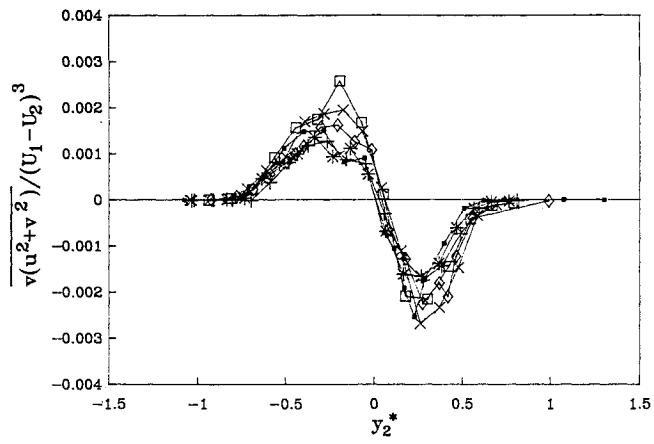

Fig. 14. The lateral convection of kinetic energy.

flows, shown in Fig. 10, is about 18.5%, very close to values reported by other investigators.[23,24] The maximum drops to 16.5% for $M_c = 0.51$ and to 15% for $M_c = 0.64$. In any given y_2^* location, especially in the high-speed side of the flow, the intensity level increases as the convective Mach number decreases and it seems that the incompressible results define the upper limit of the fluctuations. It is desirable to compare these results to those obtained at higher convective Mach numbers. However, the available results, which are measured directly at higher convective Mach numbers, are mostly obtained with the presence of recirculating flows.[12,25] These recirculating flows are returning from highly energetic reattaching regions that charge up the shear layer and produce higher intensities. An experimental effort is presently underway to provide turbulence data at higher convective Mach numbers.

Figure 11 shows the lateral turbulence intensity distributions. The general trend of turbulence extent and level are similar to those of streamwise intensities; however, with greater difference in intensity levels of subsonic[11] and supersonic cases. For the subsonic case, velocity ratio of 0.6, the maximum intensity is about 15%, which is higher than the 12–14% reported by others.[23,24] For the supersonic case, the maximum is about 11% for M_c of 0.51, dropping to below 10% for M_c of 0.64. Similar to the streamwise fluctuations, the effect of the convective Mach number is more evident in the high-speed side of the flow. The anisotropy ratio, defined as the ratio of the streamwise to lateral turbulence intensities, for the present results, is approximately 30% higher than the subsonic result of Oster and Wygnanski.

Figure 12 shows Reynolds stress distributions for the present experiments and the Oster and Wygnanski subsonic results for a velocity ratio of 0.6. The difference between the subsonic and supersonic results are similar to those of the lateral turbulence intensity case. The maximum Reynolds stress values for the supersonic cases are about 40% lower than the subsonic results. Figures 10–12 show a general trend that the level and lateral extent of both small and large scale fluctuations decrease with increasing convective Mach number in the high-speed side of the flow. The correlation coefficient R_{uv} is shown in Fig. 13 for the present experiments. For y_2^* between -0.3 and $+0.3$, the correlation coefficient is about 0.5 and dropping toward the edges of the shear layer. General trends and also maximum values are very close to those of the incompressible shear layers.[23] The convective Mach number does not seem to have any observable effect on the correlation coefficient. Based on this conclusion and the conclusions drawn from Figs. 10–12, one could conclude that the convective Mach number or compressibility is affecting both large and small scale turbulence. The effect seems to be the same order on both scales. The reduced growth rate with increased convective Mach number is due to suppression of both small and large scale mixing.

The lateral transport of kinetic energy is shown in Fig. 14 for the present experiments. General trends are similar to incompressible shear layers, but the maximum values are about 2.5 times less.[26] At any given lateral location, the level of kinetic energy transport and also the maximum levels of the transport on both sides of $y_2^* = 0$ are lower for the higher convective Mach number case. This is another explanation of the reduced growth rate for the higher convective Mach number case. These conclusions are drawn by assuming that $(U_1 - U_2)$ is the proper velocity scale. This is confirmed, for the mean flow, by the collapse of the mean flow data in Figs. 4 and 6. Whether it is also the proper turbulence velocity scale needs to be explored.

Conclusions

The presented results once more substantiated the effects of convective Mach number on the growth and entrainment rates of shear layers. The mean velocity profiles of the present experiments and subsonic and supersonic results from other experiments were investigated to find the proper velocity and length scales to collapse the data. Using either the momentum thickness with a convective Mach number dependent linear transformation or vorticity thickness to nondimensionalize the lateral scale, the mean velocity profiles were found to collapse. To confirm the generality of this transformation, more reliable mean velocity data is needed for M_c greater than 1. Comparing the results for the two convective Mach number cases of the present experiments show a definite trend. As the convective Mach number is increased, levels of streamwise and lateral turbulence fluctuations, shear stress, and transport of kinetic energy in the lateral direction are decreased, but the correlation coefficient level does not change. This seems to suggest that the level of both large and small scale turbulence fluctuations is reduced as the convective Mach number is increased. This also seems to suggest that the reduction of shear-layer growth rate with increased convective Mach number is due to a reduction in both small and large scale mixing. Since the two convective Mach numbers used in these experiments were relatively close, it is desirable to conduct similar work with higher convective Mach numbers.

Acknowledgments

The support of ONR under Contract N00014-87-K-0169, with Dr. S. G. Lekoudis as the Technical Monitor, is gratefully acknowledged. We also acknowledge the partial support of NASA Lewis Research Center under Contract NAG 3-764, with Drs. E. J. Mularz and K. B. Zaman as the Technical Monitors. The support of AARL staff and two colleagues, Bassam A./K. Abu-Hijleh and Daniel E. Erwin, is very much appreciated.

References

[1]Birch, S. F. and Eggers, J. M., "A Critical Review of the Experimental Data for Developed Free Shear Layers," *Free Turbulent Shear Flows*, NASA SP-321, 1972, pp. 11-40.

[2]Brown, G. L. and Roshko, A., "On Density Effects and Large Structure in Turbulent Mixing Layers," *Journal of Fluid Mechanics*, Vol. 64, 1974, pp. 775-816.

[3]Papamoschou, D. and Roshko, A., "Observations of Supersonic Free Shear Layers," AIAA Paper 86-0162, 1986.

[4]Chinzei, N., Masuya, G., Komuro, T., Murakami, A., and Kudou, K., "Spreading of Two-Stream Supersonic Turbulent Mixing Layers," *Physics of Fluids*, Vol. 29, No. 5, 1986, pp. 1345-1347.

[5]Messersmith, N. L., Goebel, S. G., Frantz, W. H., Krammer, E. A., Renie, J. P., Dutton, J. C., and Krier, H., "Experimental and Analytical Investigations of Supersonic Mixing Layers," AIAA Paper 88-0702, 1988.

[6]Samimy, M. and Elliott, G. S., "Effects of Compressibility on the Structure of Free Shear Layers," AIAA Paper 88-3054A, 1988.

[7]Ragab, S. A. and Wu, J. L., "Instabilities in the Free Shear Layer Formed by Two Supersonic Streams," AIAA Paper 88-0038, 1988.

[8]Zhuang, M., Kubota, T., and Dimotakis, P. E., "On the Stability of Inviscid, Compressible Free Shear Layers," *Proceedings of 1st National Fluid Dynamics Congress*, Cincinnati, OH 1988, pp. 768-773.

[9]Bogdanoff, D. W., "Compressibility Effects in Turbulent Shear Layers," *AIAA Journal*, Vol. 21, June 1983, pp. 926-927.

[10]Schlichting, H., *Boundary Layer Theory*, 6th Ed., McGraw-Hill, 1964, pp. 689-690.

[11]Oster, D. and Wygnanski, I., "The Forced Mixing Layer Between Parallel Streams," *Journal of Fluid Mechanics*, Vol. 123, 1982, pp. 91-130.

[12]Petrie, H. L., Samimy, M., and Addy, A. L., "Compressible Separated Flows," *AIAA Journal*, Vol. 24, 1986, pp. 1971-1978.

[13]Dziomba, B. and Fiedler, H. E., "Effect of Initial Conditions on Two-Dimensional Free Shear Layers," *Journal of Fluid Mechanics*, Vol. 152, 1985, pp. 419-442.

[14]Browand, F. K. and Latigo, B. O., "Growth of the Two-Dimensional Mixing Layer from a Turbulent and Nonturbulent Boundary Layer," *Physics of Fluids*, Vol. 22, 1979, pp. 1011-1019.

[15]Ikawa, H. and Kubota, T., "Investigation of Supersonic Turbulent Mixing Layer with Zero Pressure Gradient," *AIAA Journal*, Vol. 13, 1975, pp. 566-572.

[16]Samimy, M. and Abu-Hijleh B. A./K., "Performance of LDV with Polydisperse Seed Particles in High Speed Flows," *Journal of Propulsion and Power*, Vol. 5, No. 1, 1989, pp. 21-25.

[17]Petrie, H. L., Samimy, M., and Addy, A. L., "Laser Doppler Velocity Bias in Separated Turbulent Flows," *Journal of Experiments in Fluids*, Vol. 6, 1988, pp. 80-88.

[18]Samimy, M. and Langenfeld, C. A., "An Experimental Study of Isothermal Swirling Flows in a Dump Combustor," *AIAA Journal*, Vol. 26, Dec. 1988, pp. 1442-1449.

[19]Johnson, D. A. and Rose, W. C., "Laser Velocimeter and Hot-Wire Anemometer Comparison in a Supersonic Boundary Layer," *AIAA Journal*, Vol. 13, 1975, pp. 512-515.

[20]Smits, A. J., Alving, A. E., Smith, R. W., Spina, E. F., Fernando, E. M., and Donovan, J. F., "A Comparison of the Turbulence Structure of Subsonic and Supersonic Boundary Layers," *Proceedings of the 11th Symposium on Turbulence*, Univ. of Missouri, Rolla, MO, Oct. 1988.

[21]Samimy, M. and Abu-Hijleh, B. A./K., "Structure of Reattaching Supersonic Shear Layers," *Proceedings of 1st National Fluid Dynamics Congress*, Part 2, July 25-28, 1988, Cincinnati, OH, pp. 1016-1021.

[22]Smith, M. W. and Smits, A. J., "Cinematic Visualization of Coherent Density Structures in a Supersonic Turbulent Boundary Layer," AIAA Paper 88-0500, Jan. 1988.

[23]Mehta, R. D., Inoue, O., King, S. L., and Bell, J. A., "Comparison of Experimental and Computational Techniques for Plane Mixing Layers," *Physics of Fluids*, Vol. 30, 1987, pp. 2054-2062.

[24]Champagne, F. H., Pao, Y. H., and Wygnanski, I. J., "On the Two-Dimensional Mixing Region," *Journal of Fluid Mechanics*, Vol. 74, 1976, pp. 209-250.

[25]Samimy, M., Petrie, H. L., and Addy, A. L., "A Study of Compressible Turbulent Reattaching Free Shear Layers," *AIAA Journal*, Vol. 24, 1986, pp. 261-267.

[26]Wygnanski, I. and Fiedler, H., "The Two- Dimensional Mixing Region," *Journal of Fluid Mechanics*, Vol. 41, 1970, pp. 327-361.